

Original Article

Cite this article: Vitale S, Fedele L, Tramparulo FDA, and Prinzi EP (2019) Fault rocks within the blueschist metabasalts of the Diamante–Terranova unit (southern Italy): potential fossil record of intermediate-depth subduction earthquakes. *Geological Magazine* 156: 1771–1782. <https://doi.org/10.1017/S0016756819000062>


Received: 10 August 2018
Revised: 19 January 2019
Accepted: 19 January 2019
First published online: 18 March 2019

Keywords:

fault rocks; HP/LT metamorphism; palaeoseismicity; pseudotachylyte; southern Apennines – Calabria – Peloritani Terrane; ultracataclasite

Author for correspondence: Stefano Vitale,
Email: stefano.vitale@unina.it

Fault rocks within the blueschist metabasalts of the Diamante–Terranova unit (southern Italy): potential fossil record of intermediate-depth subduction earthquakes

Stefano Vitale , Lorenzo Fedele, Francesco D’Assisi Tramparulo and Ernesto Paolo Prinzi

Dipartimento di Scienze della Terra, dell’Ambiente e delle Risorse (DiSTAR), Università degli Studi di Napoli Federico II, Via Cupa Nuova Cintia 21, 80126 Napoli, Italy

Abstract

We report the first evidence of fault rocks (FRs) developed during high-pressure/low-temperature (HP/LT) subduction-related metamorphism, within quartz+epidote pods embedded in the glaucophane–lawsonite-bearing ophiolitic metabasalts of the Diamante–Terranova unit (Calabria, Italy). FRs occur as relic injections appearing as thin dark seams, locally showing an internal foliation characterized by tabular, curvilinear and meander-like shapes, and consist of very fine grains of glaucophane and titanite, locally including survivor clasts of epidote and lawsonite. Some boudinaged veins show glaucophane fibres in the boudin necks, marking a clear HP/LT syn-metamorphic origin at *c.* 30 km depth. The injected FRs can be alternatively interpreted either as pseudotachylytes or as fluidized ultracataclasites. Although subsequent recrystallization largely obliterated primary diagnostic features, the occurrence of (i) different-coloured flow streaks, characterized by alternating layers of glaucophane and titanite, (ii) well-developed flow folds and (iii) corroded epidote survivor crystals could indicate a viscous flow of molten material characterized by a non-uniform chemical composition. With this in mind, we support the hypothesis that these fine-grained veins were originally pseudotachylytes generated by the frictional melting of the glaucophane-rich layers of the Diamante–Terranova metabasalts, likely related to seismic events occurring during the Eocene along thrust faults within the subducting oceanic Ligurian lithosphere. The lack of evidence for pseudotachylyte relics in the metabasalt source rock argues for a selective preservation, largely dependent on the efficient mechanical shielding action of the stiffer quartz+epidote pods.

1. Introduction

Fault rocks such as pseudotachylytes or fault gouges are classically thought to be a record of seismic slip events (e.g. Sibson, 1975; Lin, 1996, 2008; Chester & Chester, 1998) and are consequently considered as ‘earthquake fossils’ (see Lin, 2008), whose finding can help to shed light on brittle processes occurring at various depths within the crust (e.g. Sibson, 1975; Allen, 2005; Di Toro et al. 2005a, b, 2006).

Tectonic pseudotachylytes, formed by frictional melting during coseismic localized slip along a fault (i.e. typically at 1 cm s⁻¹ to 1 m s⁻¹ slip rates; e.g. Philpotts, 1964; Sibson, 1975) are frequently associated with cataclasites and/or mylonites (e.g. Chu et al. 2012; Rowe et al. 2012; Kirkpatrick & Rowe, 2013; Wang et al. 2015), indicating that, despite being the result of frictional mechanisms, they can also form below the brittle–ductile transition within the crust. This evidence can be explained assuming episodic rapid slip events within a general framework of slow ductile deformation (e.g. Handy & Brun, 2004). At lower crustal conditions, this process can be also repeated, with alternating brittle and ductile deformation phases (e.g. Angiboust et al. 2015; Menegon et al. 2017; Behr et al. 2018; Hawemann et al. 2018; Menant et al. 2018).

Generally speaking, the relative paucity of pseudotachylyte veins in the geological record has fed a long-lasting debate (e.g. Sibson & Toy, 2006), on whether this should be ascribed to: (i) the substantial rarity of frictional melting episodes, (ii) the occurrence of mechanisms different from frictional melting during seismic events in subduction environments, such as dehydration embrittlement, especially in a fluid-rich context such as the subduction channel, resulting in the development of different types of fault rocks (FRs) (e.g. mineral veins; Angiboust et al. 2011), or (iii) the intrinsic difficulty of pseudotachylyte preservation (e.g. Kirkpatrick et al. 2009; Price et al. 2012; Kirkpatrick & Rowe, 2013). In addition, pseudotachylyte occurrences are not uniformly distributed in the various lithotypes. According to the original estimates reported by Sibson & Toy (2006), less than 3 % of the total known pseudotachylytes are hosted in mafic blueschist/eclogite facies rocks, most of them being rather hosted within quartzo-feldspathic

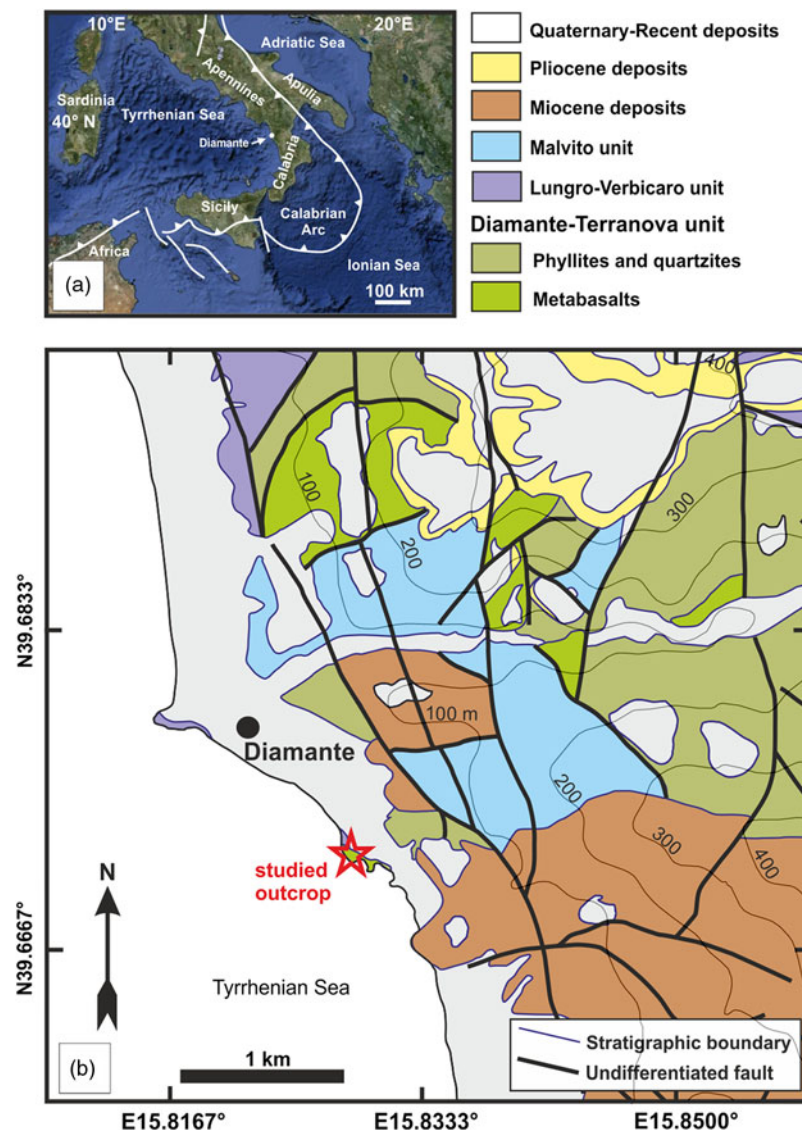


Fig. 1. (Colour online) (a) Satellite image showing the Diamante location in the framework of the southern Apennines – Calabria Peloritani Terrane system (with the position of the inferred orogenic front). (b) Simplified geological map (after Fedele et al. 2018) of the Diamante area showing the location where the investigated fault rocks (FRs) crop out (red star).

crystalline rocks (e.g. Sibson & Toy, 2006; Kirkpatrick et al. 2012; Rowe et al. 2012; Di Vincenzo et al. 2013; Wang et al. 2014, 2015; Ferré et al. 2015; Zheng et al. 2016; Stewart & Miranda, 2017; Wex et al. 2017). However, in recent years the study of FRs hosted within subducted ophiolites that experienced high-pressure/low-temperature (HP/LT) metamorphism has become a significant focus of research, and findings of pseudotachylytes in blueschist/eclogite rocks have significantly increased in number (e.g. Austrheim & Boundy, 1994; Austrheim & Andersen, 2004; Rowe et al. 2005; John & Schenk, 2006; Andersen et al. 2008, 2014; John et al. 2009; Deseta et al. 2014a, b; Magott et al. 2016, 2017; Scambelluri et al. 2017).

In this paper, we present the first evidence of FR relics, interpreted as pseudotachylyte injections, for a metaophiolite unit (Diamante–Terranova unit; DIATU) exposed in northern Calabria. This finding can contribute to shedding additional light on the factors influencing the genesis and preservation in the geological record of pseudotachylytes, to better understanding the ductile and brittle deformation mechanisms acting under the HP/LT conditions

experienced by the DIATU during the subduction–exhumation process, and the palaeoseismic activity of Calabria, possibly witnessing for a long-lived activity (at least since the Eocene and currently ongoing) for this part of the orogenic chain.

2. Geological setting

In northern Calabria, the exposed thrust-sheet pile includes some slivers of HP/LT metaophiolites. These are embedded between Palaeozoic continental crust and related Mesozoic cover rocks (Calabria–Peloritani Terrane) on the top, and Triassic–Miocene continental margin successions (Apennine Platform units; Adria plate) at the bottom (e.g. Bonardi et al. 2001; Iannace et al. 2007; Vitale & Ciarcia, 2013; Fedele et al. 2018; Vitale et al. 2019). The Diamante–Terranova unit (Cello et al. 1996; Fedele et al. 2018 and references therein), cropping out mainly in the Diamante area (on the Tyrrhenian side of northern Calabria; Fig. 1), is characterized by Jurassic metabasalts and a Cretaceous metasedimentary cover. It experienced a tectonic burial within a subduction channel,

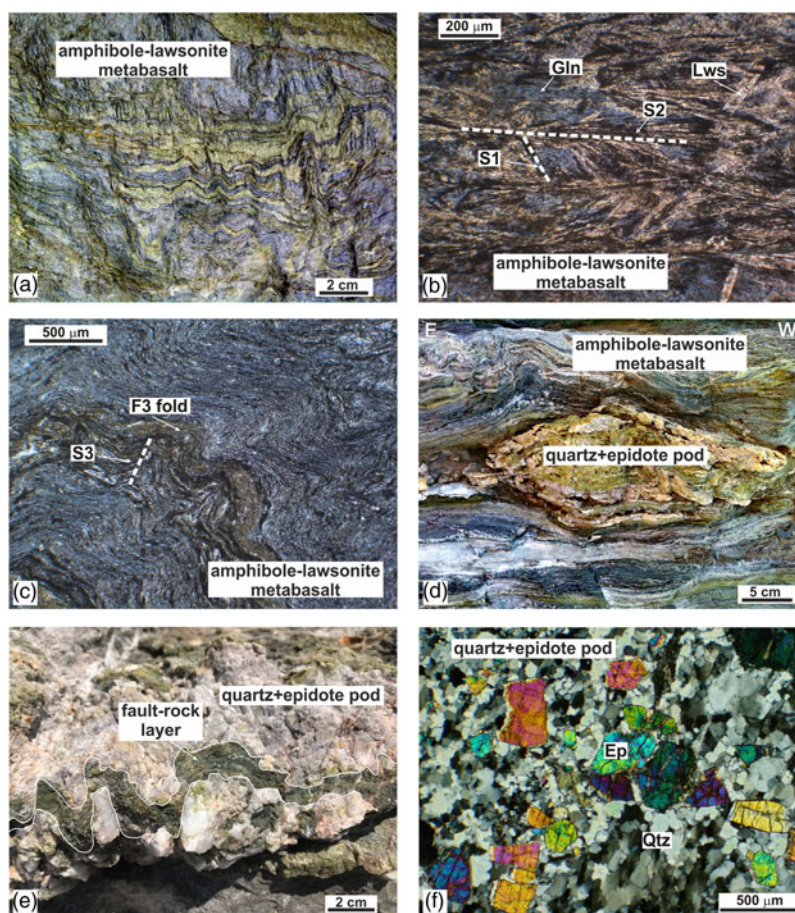


Fig. 2. (Colour online) (a) Representative field photograph of the glaucophane–lawsonite-bearing Diamante blueschist metabasalts. Plane polarized light view photomicrographs of the Diamante blueschist metabasalts: (b) S1 and S2 foliations; (c) F3 fold and related S3 foliation. (d) Field photograph of a quartz+epidote pod embedded within the Diamante metabasalts; (e) pod hosting a non-planar fracture filled with a meander-like fault rock layer. (f) Representative crossed polarized light view photomicrograph of a quartz (Qtz)+epidote (Ep) pod.

following the subduction of the Ligurian oceanic lithosphere beneath the Calabria–Peloritani Terrane (CPT).

The DIATU metabasalt rocks suffered a metamorphic cycle peaking at $T = 350\text{--}390\text{ }^{\circ}\text{C}$ and $P = 0.8\text{--}1.1\text{ GPa}$ during the Eocene ($46.7 \pm 0.4\text{ Ma}$; Shimabukuro et al. 2012), developing a mineral assemblage mainly consisting of glaucophane, lawsonite, chlorite and pumpellyite, with accessory quartz, titanite, albite and apatite (Fedele et al. 2018). At the outcrop scale, metabasalts generally appear as well-foliated rocks defined by alternating blue and green layers (Fig. 2a) consisting of glaucophane+lawsonite- and lawsonite+chlorite+pumpellyite-dominated assemblages, respectively. The tectonic evolution was accompanied by a complex ductile and brittle polyphase deformation (Fedele et al. 2018). The early ductile deformation stage, defined by three deformation phases (D1–D2–D3), occurred close to the HP/LT metamorphic peak, during the tectonic exhumation of the DIATU within the subduction channel. The widespread occurrence of syn-kinematic lawsonite crystals associated with the ductile deformation allowed Fedele et al. (2018) to estimate the pure and simple shear strain components by means of a vorticity analysis. The D1–D2 deformation was characterized by ductile non-coaxial strain with a dominant flattening component, developing an S1 foliation transposed into a main S2 crenulation cleavage (Fig. 2b). The late folding (D3) developed only a weak S3 crenulation cleavage (Fig. 2c). The subsequent deformation stages (D4–D5–D6) occurred at shallower crustal levels without metamorphic recrystallization.

Metabasalts of the DIATU embed quartz+epidote pods up to 10 cm thick, originally developed as veins during the D1 deformation stage, and subsequently folded and boudinaged (Fig. 2d). At the mesoscale observation, pods host meander-like thin dark seams of very fine-grained material enclosed within fractures, locally displaying tabular, curvilinear and meander-like shapes (Fig. 2e), identified as FR after optical and scanning electron microscope observations (see below).

3. Microstructural observations of the DIATU pods

Several samples of the quartz+epidote pods, embedded within the DIATU metabasalts and hosting the investigated FRs, were collected and subjected to detailed microstructural and petrographic investigations. Selected samples were then investigated using optical microscope and a JEOL JSM-5310 Scanning Electron Microscope (SEM) at the laboratories of the DiSTAR (Napoli). Backscattered electron (BSE) images were acquired during SEM observations, and the mineral phases were qualitatively analysed by EDS (energy dispersive spectrometry) using an Oxford Instruments Microanalysis Unit equipped with an INCA X-act detector. Measurements were performed with an INCA X-stream pulse processor using a 15 kV primary beam voltage, 50–100 μA filament current, variable spot sizes and 50 s of acquisition time. Observations at both the optical microscope and at the SEM revealed the existence of several different structures within the

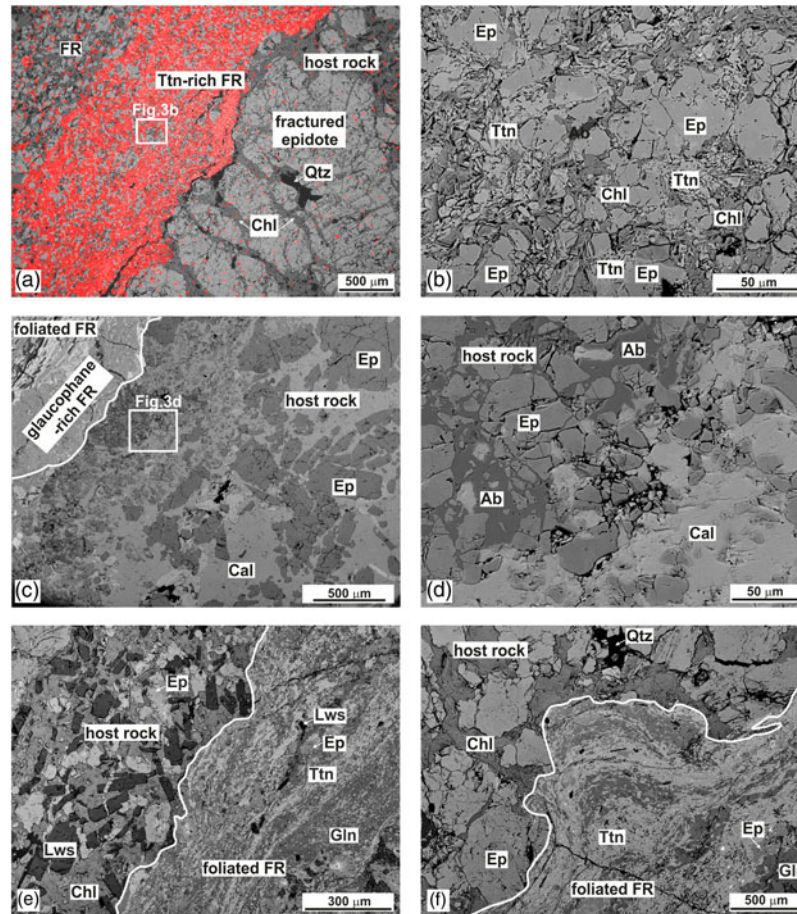


Fig. 3. (Colour online) Representative backscattered electron (BSE) scanning electron microscope (SEM) images of the investigated quartz+epidote pod samples hosting fault rock (FR) relics recovered in the DIATU metabasalts. (a) Red false colours highlighting Ti concentrations discriminating titanite (Ttn) from survivor clasts within a FR at the contact with a large fractured epidote crystal (with fractures filled with chlorite (Chl) and quartz (Qtz)) of the host pod (sample DIA17a). (b) Close-up view of the previous picture, showing high concentrations of survivor clasts (mainly crystals of epidote, Ep and Chl) embedded in a FR matrix dominated by titanite. (c) Vein showing a decrease in grain size approaching the contact with the FR, which features both a glaucophane-rich and a foliated facies (sample DIA17b; Cal = calcite). (d) Close-up view of the previous picture showing clasts of Ep within a cement made of Cal and albite (Ab). (e, f) Focus on a contact [note the jagged indented outline, especially in (f)] between the quartz+epidote pod host rock and a foliated FR (sample DIA17b; Gln = glaucophane).

investigated pod samples, including relics of fine-grained FRs and various types of late structures such as quartz-mylonites, boudins and minor thrust faults. These are described in detail in the following sections.

3.a. Host rock

Pods generally consist of variably comminuted (up to a few mm in size) broken crystals of epidote with subordinate lawsonite and glaucophane (Figs 2f, 3c–f, 4a–d, 5a–c and 6a–c) embedded by quartz and lesser calcite, chlorite and albite (Fig. 3d). The abundant quartz suggests that pods are veins related to fluid-induced brecciation (hydrofracturing). The average crystal size of broken epidote crystals is only locally observed to quite regularly decrease towards the contact with the FR relics (Fig. 3c), whereas more frequently no systematic variation of the grain size can be observed (Fig. 3e, f).

3.b. Fault rock relics

Relics of FRs typically appear as yellowish-brown to brown-dark films when observed under the optical microscope in plane polarized light view (Figs 4, 6). FRs show different degrees of

foliation development, including: (i) no foliation (Fig. 4a), (ii) a weakly developed foliation (Fig. 4b–d) and (iii) a well-developed foliation (Fig. 6). Types (i) and (ii) contain survivor clasts more or less homogeneously dispersed in a finer matrix. FRs show variably coloured streaks, generally mantling asperities of the host rock (Figs 4, 6). Locally, FRs form flow folds that can be observed both in the main vein (Fig. 4c) and in small injection veins intruding in the host rock (Fig. 4d). More frequently, FRs show a well-marked foliation that is particularly evident at the SEM, defined by layers of different mineral composition (different tones of grey) and alignment of survivor clasts (Fig. 5a–f). These latter, generally formed by broken crystals of epidote, occur in variable amounts, occasionally reaching extremely abundant concentrations (approximately ~50 vol. %; Fig. 3a, b) and locally forming lens/ribbon-shaped aggregates (Fig. 5c–e). Less common lawsonite survivor clasts are occasionally boudinaged and show evidence for growth of glaucophane fibres in the necks (Fig. 5e).

High-magnification BSE SEM images of foliated FRs reveal the presence of very fine crystals (<10 µm) of glaucophane and titanite, typically forming regular alternations of monomineralic layers (respectively darker grey and lighter grey; e.g. Fig. 5f). Crystals generally display a relatively well-formed euhedral habit, although we also observed some subhedral to anhedral shapes (Fig. 5f).

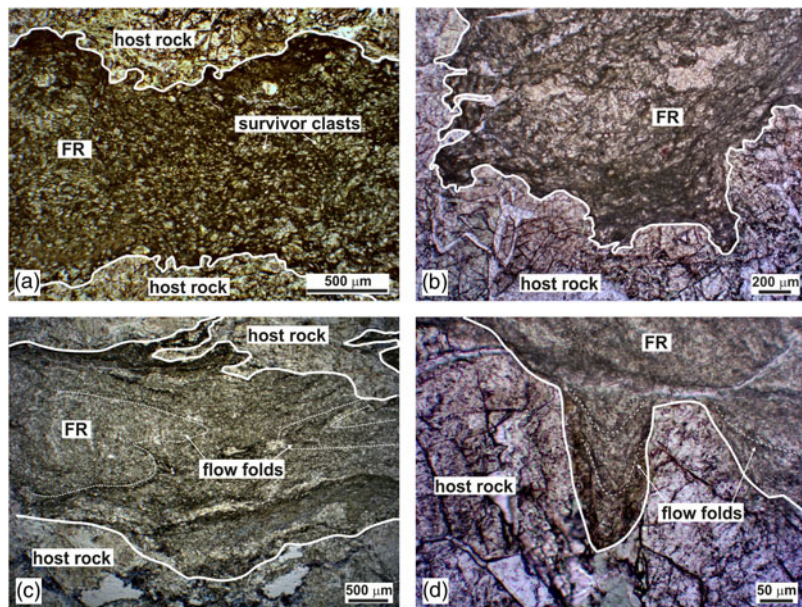


Fig. 4. (Colour online) Representative plane polarized light view photomicrographs of the investigated quartz+epidote pod samples hosting fault rock (FR) relics recovered in the DIATU metabasalts (sample DIA17), showing (a) high concentrations of survivor clasts; (b) amoeboid injections within host rock; (c), weakly foliated appearance with flow folds; and (d) small injection veins within the host rock.

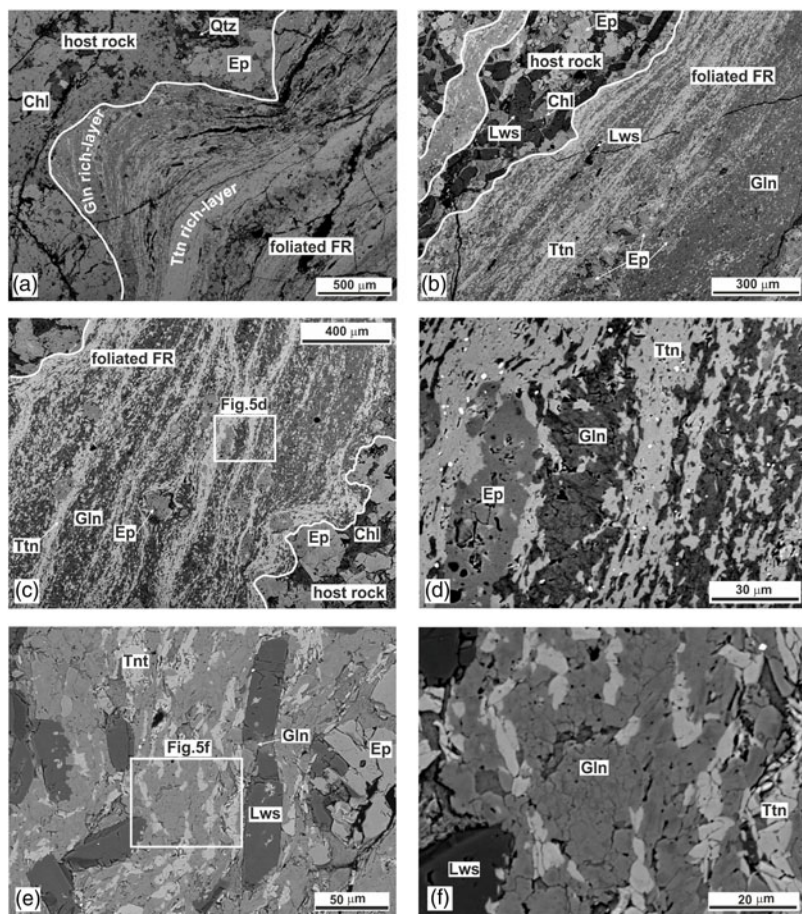


Fig. 5. Representative BSE SEM images illustrating some characteristic textural features of the investigated fault rock (FR) relics hosted in the quartz+epidote pod samples recovered in the DIATU metabasalts. (a) Foliated FR consisting of very small crystals of titanite (Ttn, light grey), and glaucophane (Gln, darker grey), forming a festoon-like structure mantling host rock asperities [the same structure is shown in (c) at the optical microscope] (DIA17b; Chl = chlorite, Qtz = quartz). (b) Foliated FR embedding layers of the host rock made of crystals of lawsonite (Lws), epidote (Ep) and Gln (DIA17b). (c) Foliated FR showing sparse Ep survivor clasts (sample DIA17) close to the contact with the host rock (right end), with white rectangle indicating the area of the enlarged view of (d), showing the FR microcrystalline texture. (e) Foliated FR showing lawsonite (Lws) survivor clasts (sample DIA17), with white rectangle indicating the area of the enlarged view of (f), where the microcrystalline texture of the FR is again evidenced.

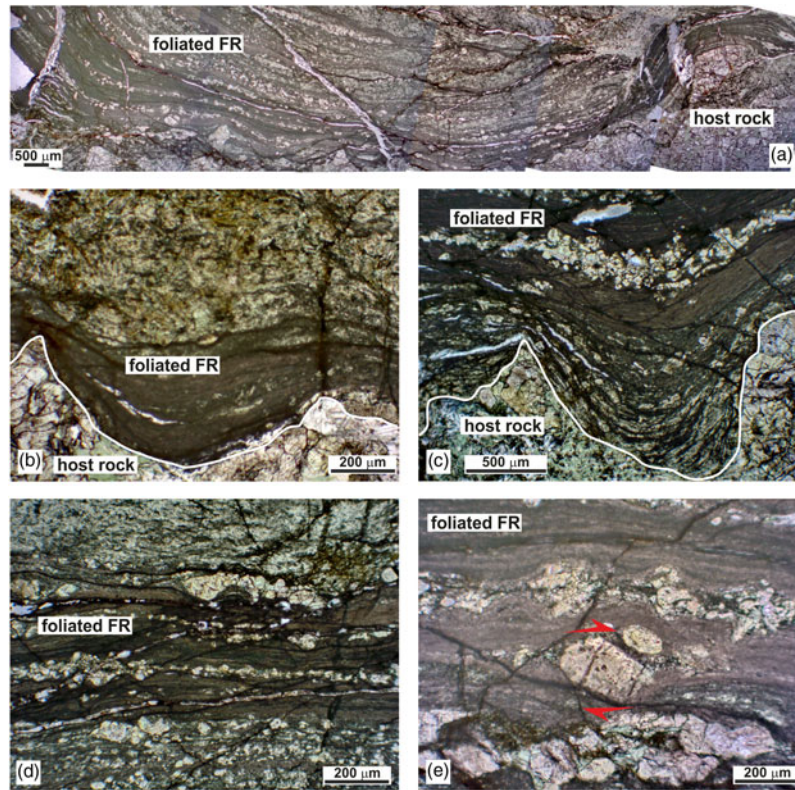


Fig. 6. (Colour online) Representative plane polarized light view photomicrographs illustrating some characteristic textural features of the investigated foliated fault rock (FR) relics hosted in the quartz+epidote pod samples recovered in the DIATU metabasalts (sample DIA17b). (a) Low-magnification view of a foliated FR seam. (b, c) Festoon-like structures of foliated FR (flow fold) filling embayments of the host rock (with higher concentrations of epidote survivor clast layers in (c)). (d) Foliated FR with very abundant layers of epidote survivor clasts. (e) Close-up view of a mantled epidote survivor clast indicating a dextral sense of shear.

Crystal aggregates typically form thin anastomosing seams wrapping epidote survivor clasts and mantling host rock asperities, locally resulting in festoon-like structures (flow folds) within host rock embayments (Fig. 5a) or amoeboid injection structures (Fig. 4b). The dark levels within foliated FRs observed with the optical microscope (e.g. Fig. 6c) proved to be enriched in titanite crystals when analysed at the SEM (Fig. 5a). Survivor clasts of epidote are commonly mantled by fine-grained fragments, occasionally showing a δ symmetric shape (Passchier & Trouw, 1996), indicating a simple shear component during the emplacement of the FR (Fig. 6e).

3.c. Late structures

Several late deformation structures, clearly following the development of the FRs, can be locally observed both in the pod and FRs. Quartz is locally deformed, with fine to coarse crystals (up to 200 μm) showing elongate shapes and a typical curved mylonitic foliation (Fig. 7a). The largest of such quartz crystals also display undulose extinction and the development of subgrains (Fig. 7b).

FRs are locally boudinaged, with necks separated by glaucophane fibres and pinch and swell structures (Fig. 7c). In addition, FRs are also observed to be deformed by small reverse faults with slickenside fibres of calcite and quartz (Fig. 7d).

4. Discussion

4.a. The DIATU fault rock relics: pseudotachylytes or ultracataclasites?

Though appearing only in very small occurrences within the investigated quartz+epidote pods, the studied relics of FRs possibly

represent the repository of some interesting clues regarding the deformation mechanisms affecting the DIATU rocks during the subduction–exhumation process. Their nature as injection vein relics of FRs is evidenced by their peculiar mineral composition consisting of very fine-grained glaucophane and titanite crystals, indicative of bulk source rock composition different from that of the host quartz+epidote pods (where such mineral phases are largely subordinate). Such FR injections could be interpreted as representing (i) mylonites, (ii) melt-originated pseudotachylytes or (iii) fluidized ultracataclasites. Since no shear plane was observed (FRs are clearly injected within fractures) and no ductile mechanism can explain the high concentration of titanite within the FRs with respect to the metabasalt photolith, hypothesis (i) can be easily discarded.

Although there is a substantial genetic difference between tectonic pseudotachylytes and ultracataclasite veins (including crush-origin pseudotachylyte-like veins; e.g. Lin, 1996, 2008; Wenk *et al.* 2000; Janssen *et al.* 2010a, b; Lin *et al.* 2013) representing the injection of a fault gouge into fractures cross-cutting the slip plane of a fault zone, assessing whether the observed FRs should be considered as pseudotachylyte or fluidized ultracataclasites is not straightforward.

A first-level difficulty is simply related to the overall similar appearance of the two types of rocks, including the fact that both have been demonstrated to form veins with similar aspect ratios (~ 0.2 ; Rowe *et al.* 2012), and that amorphous material can also occur in ultracataclasites (likely formed by mechanochemical effects during the comminution process; e.g. Ozawa & Takizawa, 2007; Pec *et al.* 2012). Furthermore, pseudotachylytes and ultracataclasites are commonly associated with and gradational to each

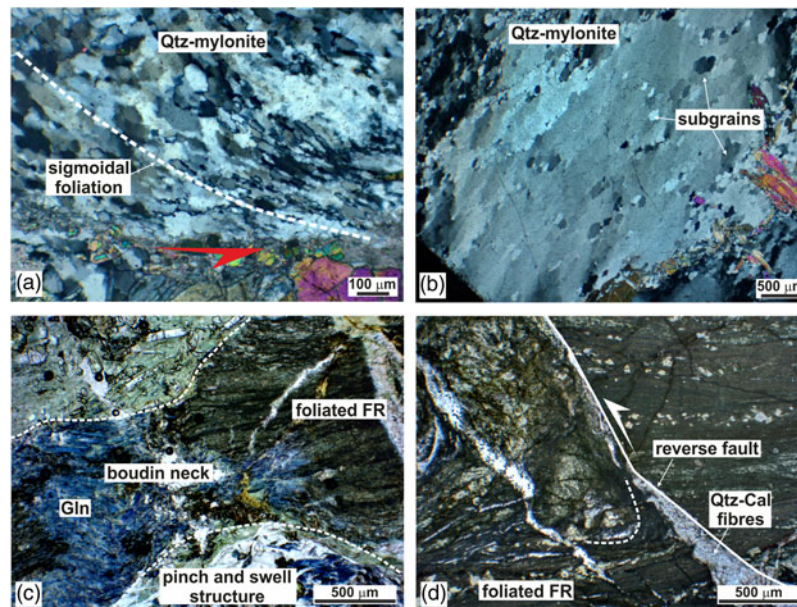


Fig. 7. (Colour online) Representative photomicrographs illustrating some characteristic late structures observed in the investigated quartz+epidote pod samples hosting fault rock (FR) relics recovered in the DIATU metabasalts (sample DIA17). Crossed polarizers view of a quartz (Qtz)-mylonite showing (a) sigmoidal foliation and (b) formation of subgrains (high-interference colour crystals are epidote crystals). Plane polarized light view of (c) boudinaged FR with glaucophane (Gln) fibres growing in the neck, (d) reverse-fault deforming the foliated FR (Cal = calcite).

other (as well as with ultramytonites), so they might be indistinguishable from each other even at the microscope scale.

This finally brings us to the core of the problem, as the presence of (metastable) glass and/or ultrafine-grained material makes both pseudotachylytes and ultracataclasites extremely prone to obliteration (though sometimes glass can be well preserved; e.g. Andersen & Austrheim, 2006; Andersen et al. 2008) via recrystallization, alteration, hydration and deformation (see Kirkpatrick & Rowe (2013) for an exhaustive synthesis). As a consequence, the most diagnostic features of both pseudotachylytes (i.e. chilled margins, spherulites, dendritic/skeletal crystals suggesting rapid quenching of a melt) and ultracataclasites (i.e. ultrafine rock fragments marking a clear crush origin) are not always clearly recognizable. The latter is likely the case of the investigated DIATU FR relics. In fact, they have recrystallized in blueschist facies conditions, as indicated by: (i) presence of glaucophane; (ii) host quartz+epidote pods formed in similar HP/LT conditions with respect to enclosing metabasalts (i.e. $T = 350\text{--}390\text{ }^{\circ}\text{C}$ and $P = 0.8\text{--}1.1\text{ GPa}$, corresponding to a depth of $\sim 30\text{ km}$; Fedele et al. 2018); (iii) some FRs being locally boudinaged with glaucophane fibres in the neck (Fig. 6c). In addition, the host quartz+epidote pods likely also experienced a complex deformation history, as testified by the occurrence of ductile and brittle late structures. Pods clearly pre-date the FR relics, as the latter are hosted within them as injection veins (Figs 3e, f, 4c–f, 5a–c). A subsequent ductile deformation stage is also evident, as recorded by dynamic recrystallization of quartz crystals (Fig. 4a, b). The evidence that FR veins do not cut the quartz-mylonites suggests that the ductile process was also subsequent to the FR injections. Hence, this complex history of recrystallization and deformation has likely overprinted the primary textural features of the investigated FRs. However, a possibly diagnostic feature is represented by the common presence of a clear distinction between titanite- and glaucophane-dominated layers (e.g. Figs 3e, f, 5a–d). This could be achieved through flow differentiation during melt injection, consistent with the common

presence of flow structures (e.g. Figs 4e, f, 5a, 6b, c), suggesting non-equilibrium melting processes or lack of melt homogenization (e.g. Chu et al. 2012; Kirkpatrick & Rowe, 2013; Deseta et al. 2014a, b). Flow banding seems evident even at the optical microscope scale, as also highlighted by the common wrapping of epidote survivor clasts, represented not only by isolated clasts (e.g. Figs 3b, 5d), but also by boudinaged levels (Fig. 6d, e).

In this framework, the occurrence of flow streaks with different colour and composition could be related to viscous flow of molten material characterized by a non-uniform chemical composition (e.g. Toyoshima, 1990). Pseudotachylyte streaks frequently form tight to isoclinal folds, with a geometry of similar-type folds (flow folds; Berlenbach & Roering, 1992; O'Hara, 2001; Theunissen et al. 2002). In the analysed FRs, the flow foliation is curved in the central part of the vein, and becomes parallel to the vein margin, as observed in some lateral 'subsidiary' injection veins (Fig. 4e, f) or in some embayments within the host rock (Figs 3f, 5a, 6b, c).

Although foliation is a feature commonly ascribed to pseudotachylytes, it should however be noted that in some cases it has also been reported for ultracataclasites (e.g. Magloughlin & Spray, 1992; Chester & Chester, 1998; Cashman & Cashman, 2006; Kirkpatrick & Rowe, 2013; Wang et al. 2015), so it cannot be considered to be a fully diagnostic feature for melt-originated FRs. However, well-developed flow folds, such as those observed in the analysed FRs, are never reported for ultracataclasites, which are more likely to display a homogeneous mineral composition, rather than a well-developed compositional banding like that observed for the DIATU FRs.

Relic survivor clasts (as well as their size distribution; e.g. Ray, 2004; Lin, 2008; Price et al. 2012) can be of some use in discriminating between pseudotachylytes and ultracataclasites, but similarly do not provide unequivocal clues in this sense. The presence of embayed clasts, testifying to incomplete melting of fragments from the source rock, is generally taken as supporting a melting-related origin for these FRs (e.g. Kirkpatrick & Rowe, 2013). The most

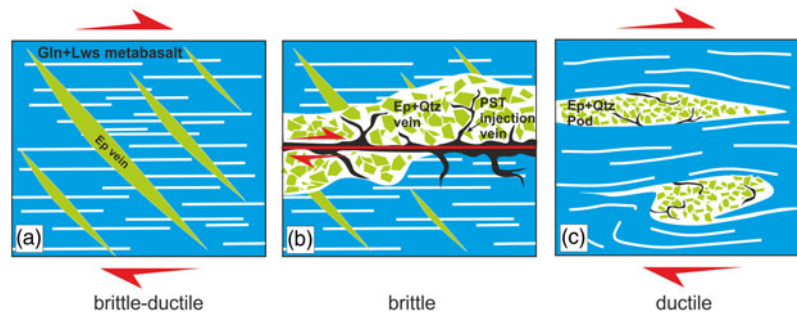


Fig. 8. (Colour online) Cartoon showing the reconstructed evolution for the investigated DIATU pseudotachylytes (PST). Gln = glaucophane; Lws = lawsonite; Ep = epidote; Qtz = quartz.

common survivor clasts observed in the investigated FRs are instead from the host quartz+epidote pods, showing rounded and embayed morphologies (e.g. Figs 3b, 5d, e, f). This feature is in contrast to the typical angular shape expected for a clast within an ultracataclasite. The corroded appearance of the epidote crystal in Figure 5d could thus be taken as evidence of a partially molten survivor clast that reacted with an infiltrating melt. Similarly, the lawsonite crystals of Figure 5e, as well as the few subhedral/anedral crystals of glaucophane and titanite surrounded by euhedral crystals in the FR vein of Figure 5f, can be interpreted as partially melted relics dragged from the source metabasalt.

In the light of the above evidence, we think that the DIATU FRs can be more confidentially interpreted as pseudotachylytes, rather than ultracataclasites. In any case, it should be noted that even if the investigated FRs (or at least some of them) are considered to have originated from a granular flow rather than from a quenching melt, their textural features are still consistent with a process related to high slip rates. The genesis of ultracataclasite injections has indeed been ascribed to at least three different mechanisms: (i) slow deposition of clay minerals-rich materials transported by hydrothermal fluids; (ii) slow intrusion along fractures during aseismic periods (e.g. Lin, 1996, 2008, 2011; Bjørnerud, 2010); and (iii) fast intrusion during seismic slip (e.g. Otsuki et al. 2003; Rowe et al. 2005, 2012; Ujiie et al. 2007; Brodsky et al. 2009; Bjørnerud, 2010; Lin, 2011; Lin et al. 2013). In the DIATU case, mechanism (i) seems unlikely, as a slow flow within a hydrothermal fluid would probably have enriched the veins in clay minerals due to density sorting. Similarly, a slow flow such as is required for mechanism (ii) also seems unconvincing, as it could not allow the sharp separation between glaucophane and titanite observed in some of the investigated FRs. On this basis, the only viable mechanism is (iii), and so we conclude that the investigated FR relics have to be considered as evidence of processes acting at seismic rates.

4.b. A genetic model for the DIATU pseudotachylytes

A model summarizing the overall deformation evolution explaining the genesis of the DIATU pseudotachylyte veins is suggested in Figure 8, based on the evidence presented in the previous section. The earliest deformation stage was mainly in the brittle–ductile regime, during HP/LT metamorphism (Fig. 8a), characterized by low strain rates (e.g. $10^{-12}/10^{-10}$ s $^{-1}$; Spray, 2010), with the development of the glaucophane+lawsonite+chlorite+pumpellyite metabasalt assemblage and the epidote veins. The subsequent activation of a thrust fault (Fig. 8b), defined by very high slip rates ($\sim 10^{-1}/10^6$ s $^{-1}$; Spray, 2010), caused the transition to a dominant

brittle deformation style, producing quartz+epidote veins by means of hydraulic fracturing, accompanied by melting, along the fault plane, of glaucophane and titanite in the metabasalts, locally producing pseudotachylyte injection veins. The evidence that the quartz-mylonites do not host pseudotachylytes and the absence of multiple generations of pseudotachylytes suggest that, at least in the analysed rocks, there was no multiple alternation of brittle (fast slip events) and ductile (normal strain rate) deformation stages.

The peculiar biminerale composition of the DIATU pseudotachylytes supports the idea that melting must have been extremely selective, as it did not occur either in the epidote veins or in the green lawsonite+chlorite+pumpellyite-dominated layers of the metabasalt, but it only affected the glaucophane-dominated (including diffuse titanite accessory crystals) metabasalt layers. This could be explained assuming a decrease of effective normal stress over the fault plane, which hence lowered the frictional heat (Passchier & Trouw, 1996), due to the presence of high volumes of fluids. Such fluids can be related to the release of dehydration water by the H $_2$ O-rich green layers of the host metabasalt (also including abundant lawsonite), which was also responsible for the development of the aforementioned quartz+epidote veins and fluid-induced brecciation processes. On the other hand, the relatively low porosity and lower water content of glaucophane-rich layers likely allowed the build-up of the effective normal stress, eventually leading to melt generation.

In the successive deformation stages, melt formerly solidified as glass recrystallized under HP/LT conditions to very tiny crystals of glaucophane and titanite. Recrystallization did not erase the original flow banding, which is still evident in the form of differently coloured layers, flow folds, festoon-like structures and minor injections within the host rock. The following deformation phases, characterized by dominant flattening and minor simple shear (Fedele et al. 2018), produced (i) the observed pods, from folding and boudinage of the previous quartz+epidote veins, (ii) the quartz-mylonites, from the ductile deformation of the quartz cement of the veins and (iii) the boudinage of the pseudotachylyte veins, with the growth of glaucophane crystals in the necks. Since the studied pseudotachylytes formed during the ductile deformation phases D1–D3 of the HP/LT metamorphic event, a model assuming that fault zone shear melting was preceded and/or followed by mylonitic deformation (Passchier & Trouw, 1996; Takagi et al. 2000), commonly invoked to suggest a genetic linkage between pseudotachylytes and associated ductile structures, seems far from convincing in the DIATU case. It is more likely that brittle rapid slip events occurred within a general framework of slow deformation characterized by a ductile strain. As a final remark, the observation that pseudotachylyte relics a

are totally lacking in the DIATU metabasalt source rocks can possibly give some interesting clues to our understanding of the factors influencing the preservation in the geological record of such delicate FR. We indeed suggest that the selective preservation of the DIATU pseudotachylytes simply reflects the effects of significant tectonic obliteration acting concurrently with recrystallization, which must have completely erased any pseudotachylyte relic originally preserved in the DIATU metabasalts. Such obliteration did not occur in the stiffer quartz+epidote aggregates of the host pods because these must have efficiently shielded the tiny and vulnerable pseudotachylyte veins. This might suggest that the relative rarity of pseudotachylytes is largely dependent on the need for favourable conditions allowing their preservation.

4.c. Palaeotectonic implications

The present recognition of pseudotachylyte relics in the quartz+epidote pods embedded within the DIATU metabasalts offers the opportunity to increase our understanding of the seismogenic processes active along the subduction interface, and potentially within the subducting lithospheric plate.

In the southern Apennines – CPT system, the occurrence of pseudotachylyte veins has so far been reported only in southern Calabria, within the Hercynian basement of the Serre Massif, namely in greenschist/amphibolite-facies foliated meta-tonalites (Copanello locality; Caggianelli et al. 2005) and in high-grade mafic and felsic granulite-facies rocks (Curinga; Altenberger et al. 2013). As for the latter, Altenberger et al. (2013) hypothesized that pseudotachylytes resulted from deep-seated seismic events (*c.* 30 km in depth), occurring during the activity of the Curinga–Girifalco Fault (Schenk, 1980; Langone et al. 2006), within the geodynamic framework of the Eocene piling-up of CPT slivers. Our results provide evidence that pseudotachylyte veins formed at similar depth synchronously with the HP/LT metamorphic ductile deformation affecting the subducted thrust sheets during the Eocene closure of the Ligurian Ocean (e.g. Vitale & Ciarcia, 2013; Vitale et al. 2019). The recognized pseudotachylyte veins thus testify to a long-lasting intermediate-depth seismicity in the CPT/Ligurian domain, active at least from the Eocene until the presently ongoing Ionian subduction beneath Calabria, where deep to shallow earthquakes frequently occur (e.g. Castello et al. 2006). Similar evidence for early Eocene (55–46 Ma) intermediate-depth seismicity, based on the recognition of pseudotachylyte veins, has recently been reported by Scambelluri et al. (2017) for the oceanic gabbros and mantle peridotites of the Lanzo Massif, belonging to the northern sector of the Ligurian domain (though developed at much higher depths of 60–80 km, corresponding to eclogite-facies conditions of 550–620 °C at 2–2.5 GPa; e.g. Pelletier & Müntener, 2006; Debret et al. 2013).

The occurrence of pseudotachylyte veins is also reported for other Ligurian oceanic unit rocks such as those of the Alpine Corsica Schistes Lustrés (Austrheim & Andersen, 2004; Deseta et al. 2014a, b; Magott et al. 2016, 2017), a sort of analogue of the metamorphic Ligurian oceanic units exposed in the southern Apennines – CPT realm. These pseudotachylyte veins occur within thrust sheets of partially metamorphosed mantle peridotite and lower crust metagabbro enclosed by serpentinite and blueschist-eclogite facies schists (i.e. in a broadly similar context to that for the Lanzo Massif). This reinforces the idea, proposed here for the DIATU case, that recognition of medium- to high-depth pseudotachylyte veins is strongly dependent on the presence

of favourable geological conditions allowing their preservation. Interestingly, the Schistes Lustrés and the Lanzo Massif pseudotachylyte veins are so far the only two reported cases for pseudotachylyte occurrences from exhumed subducted ophiolites in the circum-Mediterranean orogenic chains.

The genesis of the Schistes Lustrés pseudotachylyte veins has been widely investigated (Austrheim & Andersen, 2004; Andersen et al. 2008, 2014; Deseta et al. 2014a, b) and ascribed to thermally activated processes (i.e. ‘thermal runaway’ or ‘thermally-induced shear instability’, controlled by rheology; e.g. Braeck & Podladchikov, 2007; John et al. 2009; Spray, 2010; Prieto et al. 2013). A similar mechanism is unlikely for the DIATU pseudotachylyte veins, which formed at much shallower depths with respect to the ~40–80 km range of the Alpine Corsica ones (based on the 1.4–2.6 GPa and 480–550 °C estimates for the metamorphic peak; Ravna et al. 2010; Vitale Brovarone et al. 2013 and references therein). It therefore seems likely that, in the DIATU case, brittle-controlled processes such as dehydration embrittlement (related to mineral composition; e.g. Green, 1995; Jung et al. 2004; Green & Jung, 2005; Jung et al. 2006; Okazaki & Hirth, 2016) were prevailing. This would also be consistent with their relatively low H₂O content (likely not exceeding 3 wt %, since glaucophane is the only hydrous phase), in contrast to the water-rich nature of the Schistes Lustrés pseudotachylytes (H₂O up to 15 wt %). In this regard, a parallel with the pseudotachylytes from the northern Ligurian domain rocks of the Lanzo Massif is no longer supported, since the genesis of the latter has been rather ascribed to the release of differential stresses accumulated in strong dry metastable rocks, likely as a consequence of the much higher depths of formation with respect to the shallower DIATU pseudotachylytes (Scambelluri et al. 2017).

5. Concluding remarks

- Relics of FRs in the HP/LT DIATU metabasalts cropping out in northern Calabria are hosted within pods mostly made of epidote+quartz crystals. At the mesoscale they appear as dark seams of millimetre- to centimetre-sized widths, locally characterized by internal foliation and displaying tabular, curvilinear and meander-like shapes.
- Microstructural observations by optical and scanning electron microscopes show that the FRs form injection veins, marked by flow folds, festoon-like and amoeboid structures. Injection veins are made by fine-grained crystals of glaucophane and titanite enclosing survivor clasts of epidote and more rarely lawsonite. These FRs show a wide variety of textures: some of them are massive with survivor clast dispersed in the matrix; more frequently they appear as foliated, with a foliation marked by alternating layers of glaucophane and titanite, or levels of survivor clasts with different grain sizes. Such textural features have been interpreted as indicative of an origin from seismic slip processes, which more likely produced a melt phase (successively quenched and recrystallized), rather than a granular cataclastic flow. The investigated FR injections are thus retained to represent pseudotachylyte (rather than ultracataclite) veins, generated by partial melting of the glaucophane-rich layers of the DIATU metabasalts.
- The DIATU pseudotachylytes were subsequently boudinaged with growth of glaucophane fibres in the necks, or cut by small reverse faults. Also the pods were subsequently deformed by ductile strain, with the development of a mylonitic foliation within the quartz crystals. This suggests that

the pseudotachylytes formed in HP/LT conditions at middle crustal depths during the Eocene burial of the DIATU within the subduction channel. Such a result is consistent with similar structures found in the continental CPT crystalline slivers in southern Calabria, related to the Eocene crustal thickening and developed at similar depths.

- No pseudotachylyte relic was found in the DIATU metabasalt source rock, suggesting that preservation of such delicate FR was possible only where this was shielded by the stiffer quartz+epidote pods.
- Our study confirms that the brittle processes associated with the formation of pseudotachylytes can be active also in a ductile environment, as indicated by the subsequent mylonite formation recorded by the DIATU quartz+epidote pods. Brittle mechanisms are triggered by specific physico-chemical conditions such as occurrence of fluids and pulsating high-strain rates, typical of subduction zones.
- The DIATU pseudotachylytes witness also for high-magnitude earthquakes associated with the Eocene subduction of this sector of the Ligurian Ocean.

Author ORCID.  Vitale Stefano 0000-0003-1952-0463

Acknowledgements. The authors wish to thank Roberto de Gennaro for skilled assistance during SEM observations. The official revisions from two anonymous reviewers and the editorial handling from the Executive Editor Olivier Lacombe greatly contributed to improving the quality of the paper, increasing its consistency and readability.

References

- Allen JL (2005) A multi-kilometer pseudotachylyte system as an exhumed record of earthquake rupture geometry at hypocentral depths (Colorado, USA). *Tectonophysics* **402**, 37–54.
- Altenberger U, Prosser G, Grande A, Günter C and Langone A (2013) A seismogenic zone in the deep crust indicated by pseudotachylytes and ultramylonites in granulite-facies rocks of Calabria (Southern Italy). *Contributions to Mineralogy and Petrology* **166**, 975–94.
- Andersen TB and Austrheim H (2006) Fossil earthquakes recorded by pseudotachylytes in mantle peridotite from the Alpine subduction complex of Corsica. *Earth and Planetary Science Letters* **242**, 58–72.
- Andersen TB, Austrheim H, Deseta N, Silkoset P and Ashwal LD (2014) Large subduction earthquakes along the fossil Moho in Alpine Corsica. *Geology* **42**, 395–8.
- Andersen TB, Mair K, Austrheim H, Podladchikov YY and Vrijmoed JC (2008) Stress release in exhumed intermediate and deep earthquakes determined from ultramafic pseudotachylyte. *Geology* **36**, 995–8.
- Angiboust S, Agard P, Raimbourg H, Yamato P and Huet B (2011) Subduction interface processes recorded by eclogite-facies shear zones (Monviso, W. Alps). *Lithos* **127**, 222–238.
- Angiboust S, Kirsch J, Oncken O, Glodny J, Monie' P and Rybacki E (2015) Probing the transition between seismically coupled and decoupled segments along an ancient subduction interface. *Geochemistry, Geophysics, Geosystems* **16**, 1905–22.
- Austrheim H and Andersen TB (2004) Pseudotachylytes from Corsica: fossil earthquakes from a subduction complex. *Terra Nova* **166**, 193–7.
- Austrheim H and Boundy TM (1994) Pseudotachylytes generated during seismic faulting and eclogitization of the deep crust. *Science* **265**, 82–3.
- Behr WM, Kotowsky AJ and Ashley KT (2018) Dehydration-induced rheological heterogeneity and the deep tremor source in warm subduction zones. *Geology* **46**, 475–8.
- Berlenbach JW and Roering C (1992) Sheath-fold-like structures in pseudotachylytes. *Journal of Structural Geology* **14**, 847–56.
- Bjørnerud M (2010) Rethinking conditions necessary for pseudotachylyte formation: observations from the Otago schists, South Island, New Zealand. *Tectonophysics* **490**, 69–80.
- Bonardi G, Cavazza W, Perrone V and Rossi S (2001) Calabria-Peloritani Terrane and Northern Ionian Sea. In *Anatomy of an Orogen: The Apennines and Adjacent Mediterranean Basins* (eds GB Vai and IP Martini), pp. 287–306. Dordrecht: Kluwer.
- Braeck S and Podladchikov YY (2007) Spontaneous thermal runaway as an ultimate failure mechanism of materials. *Physical Review Letters* **98**, 095504, doi: [10.1103/PhysRevLett.98.095504](https://doi.org/10.1103/PhysRevLett.98.095504).
- Brodsky E, Rowe K, Meneghini F and Moore JC (2009) A geological fingerprint of low-viscosity fault fluids mobilized during an earthquake. *Journal of Geophysical Research* **114**, B01303, doi: [10.1029/2008JB005633](https://doi.org/10.1029/2008JB005633).
- Caggianelli A, de Lorenzo S and Prosser G (2005) Modelling the heat pulse generated on a fault plane during coseismic slip: inferences from the pseudotachylyte of the Copanello cliffs (Calabria, Italy). *Tectonophysics* **405**, 99–119.
- Cashman SM and Cashman KV (2006) Cataclastic textures in La Grange fault rocks, Klamath Mountains, California. In *Geological Studies in the Klamath Mountains Province, California and Oregon: A Volume in Honor of William P. Irwin* (eds AW Snoke and CG Barnes), pp. 433–50. Boulder, Colorado: Geological Society of America, Special Paper no. 410.
- Castello B, Selvaggi G, Chiarabba C and Amato A (2006) CSI Catalogo della sismicità italiana 1981–2002, versione 1.1, INGV-CNT, Roma. <http://csi.rm.ingv.it/>.
- Cello G, Invernizzi C and Mazzoli S (1996) Structural signature of tectonic processes in the Calabrian Arc, southern Italy: evidence from the oceanic-derived Diamante-Terranova unit. *Tectonics* **15**, 187–200.
- Chester FM and Chester JS (1998) Ultracataclastic structure and friction processes of the Punchbowl fault, San Andreas system, California. *Tectonophysics* **295**, 199–221.
- Chu HT, Hwang SL, Shen P and Yui TF (2012) Pseudotachylyte in the Tananao Metamorphic Complex, Taiwan, occurrence and dynamic phase changes of fossil earthquakes. *Tectonophysics* **581**, 62–75.
- Debret B, Nicollet C, Andreani M, Schwartz S and Godard M (2013) Three steps of serpentinization in an eclogitized oceanic serpentinization front (Lanzo Massif-Western Alps). *Journal of Metamorphic Geology* **31**, 165–86.
- Deseta N, Andersen TB and Ashwal LD (2014a) A weakening mechanism for intermediate-depth seismicity? Detailed petrographic and microtextural observations from blueschist facies pseudotachylytes, Cape Corse, Corsica. *Tectonophysics* **610**, 138–49.
- Deseta N, Ashwal LD and Andersen TB (2014b) Initiating intermediate-depth earthquakes: insights from a HP-LT ophiolite from Corsica. *Lithos* **206–207**, 127–46.
- Di Toro G, Hirose T, Nielsen S, Pennacchioni G and Shimamoto T (2006) Natural and experimental evidence of melt lubrication of faults during earthquakes. *Science* **311**, 647–9.
- Di Toro G, Nielsen S, Pennacchioni G (2005a) Earthquake rupture dynamics frozen in exhumed ancient faults. *Nature* **436**, 1009–12.
- Di Toro G, Pennacchioni G and Teza G (2005b) Can pseudotachylytes be used to infer earthquake source parameters? An example of limitations in the study of exhumed faults. *Tectonophysics* **402**, 3–20.
- Di Vincenzo G, Rossetti F, Viti C and Balsamo F (2013) Constraining the timing of fault reactivation: Eocene coseismic slip along a Late Ordovician ductile shear zone (northern Victoria Land, Antarctica). *Bulletin of the Geological Society of America* **125**, 609–24.
- Fedele L, Tramparulo FDA, Vitale S, Cappelletti P, Prinzi EP and Mazzoli S (2018) Petrogenesis and deformation history of the lawsonite-bearing blueschist facies metabasalts of the Diamante-Terranova oceanic unit (southern Italy). *Journal of Metamorphic Geology* **36**, 691–714.
- Ferré EC, Geissmann JW, Chauvet A, Vauchez A and Zechmeister MS (2015) Focal mechanism of prehistoric earthquakes deduced from pseudotachylyte fabric. *Geology* **43**, 531–4.
- Green HW (1995) The mechanics of deep earthquakes. *Annual Reviews of Earth and Planetary Sciences* **23**, 169–213.
- Green HW and Jung H (2005) Fluids, faulting and flow. *Elements* **1**, 31–7.
- Handy MR and Brun J-P, (2004) Seismicity, structure and strength of the continental lithosphere. *Earth and Planetary Science Letters* **223**, 427–41.

- Hawemann F, Mancktelow NS, Wex S, Camacho A and Pennacchioni G (2018) Pseudotachylyte as field evidence for lower-crustal earthquakes during the intracontinental Petermann Orogeny (Musgrave Block, Central Australia). *Solid Earth* **9**, 629–48.
- Iannace A, Vitale S, D'Errico M, Mazzoli S, Di Staso A, Maiacone E, Messina A, Reddy SM, Somma R, Zamparelli V, Zattin M and Bonardi G (2007) The carbonate tectonic units of northern Calabria (Italy): a record of Apulian paleomargin evolution and Miocene convergence, continental crust subduction, and exhumation of HP-LT rocks. *Journal of the Geological Society* **164**, 1165–86.
- Janssen C, Wirth R, Lin A and Dresen G (2010a) TEM microstructural analysis in a fault gouge sample of the Nojima Fault Zone, Japan. *Tectonophysics* **583**, 101–4.
- Janssen C, Wirth R, Rybacki E, Naumann R, Kemnitz H, Wenk H-R and Dresen G (2010b) Amorphous material in SAFOD core samples (San Andreas Fault): evidence for crush-origin pseudotachylytes? *Geophysical Research Letters* **37**, doi: [10.1029/2009GL040993](https://doi.org/10.1029/2009GL040993).
- John T, Medvedev S, Rüpke LH, Andersen TB, Podladchikov YY and Austrheim H (2009) Generation of intermediate-depth earthquakes by self-localizing thermal runaway. *Nature Geoscience* **2**, 137–40, doi: [10.1038/NNGEO419](https://doi.org/10.1038/NNGEO419).
- John T and Schenk V (2006) Interrelations between intermediate-depth earthquakes and fluid flow within subducting oceanic plates: constraints from eclogite facies pseudotachylytes. *Geology* **34**, 557–60.
- Jung H, Green HW and Dobrzynetska L (2004) Intermediate-depth earthquake faulting by dehydration embrittlement with negative volume change. *Nature* **428**, 545–9.
- Jung H, Katayama I, Jiang Z, Hiraga I and Karato SI (2006) Effect of water and stress on the lattice-preferred orientation of olivine. *Tectonophysics* **421**, 1–22.
- Kirkpatrick JD, Dobson KJ, Mark DF, Shipton ZK, Brodsky EE and Stuart FM (2012) The depth of pseudotachylyte formation from detailed thermochronology and constraints on coseismic stress drop variability. *Journal of Geophysical Research* **117**, B06406, doi: [10.1029/2011JB008846](https://doi.org/10.1029/2011JB008846).
- Kirkpatrick JD and Rowe CD (2013) Disappearing ink: how pseudotachylytes are lost from the rock record. *Journal of Structural Geology* **52**, 183–98.
- Kirkpatrick JD, Shipton ZK and Persano C (2009) Pseudotachylytes: rarely generated, rarely preserved or rarely reported? *Bulletin of the Seismological Society of America* **99**, 382–8.
- Langone A, Gueguen E, Prosser G, Caggianelli A and Rottura A (2006) The Curinga-Girifalco fault zone (northern Serre Calabria) and its significance within the Alpine tectonic evolution of the western Mediterranean. *Journal of Geodynamics* **42**, 140–58.
- Lin A (1996) Injection veins of crushing-originated pseudotachylyte and fault gouge formed during seismic faulting. *Engineering Geology* **43**, 213–24.
- Lin A (2008) *Fossil Earthquakes: The Formation and Preservation of Pseudotachylytes*. Berlin, Heidelberg and New York: Springer. Lecture Notes in Earth Sciences 111.
- Lin A (2011) Seismic slip recorded in the fluidized ultracataclastic veins formed along the coseismic shear zone during the 2008 M_W 7.9 Wenchuan earthquake. *Geology* **39**, 547–50.
- Lin A, Yamashita K and Tanaka M (2013) *Journal of Structural Geology* **48**, 3–13.
- Magloughlin JF and Spray JC (1992) Frictional melting processes and products in geologic materials: introduction and discussion. *Tectonophysics* **204**, 197–206.
- Magott R, Fabbri O and Fournier M (2016) Subduction zone intermediate-depth seismicity: insights from the structural analysis of Alpine high-pressure ophiolite-hosted pseudotachylytes (Corsica, France). *Journal of Structural Geology* **87**, 95–114.
- Magott R, Fabbri O and Fournier M (2017) Polyphase ductile/brittle deformation along a major tectonic boundary in an ophiolitic nappe, Alpine Corsica: insights on subduction zone intermediate-depth asperities. *Journal of Structural Geology* **94**, 240–57.
- Menant A, Angiboust S, Monié P, Oncken O and Guigner J-M (2018) Brittle deformation during Alpine basal accretion and the origin of seismicity nests above the subduction interface. *Earth and Planetary Science Letters* **487**, 84–93.
- Menegon L, Pennacchioni G, Malaspina N, Harris K and Wood E (2017) Earthquakes as precursors of ductile shear zones in the dry and strong lower crust. *Geochemistry, Geophysics, Geosystems* **18**, 4356–74.
- O'Hara KD (2001) A pseudotachylyte geothermometer. *Journal of Structural Geology* **23**, 1345–57.
- Okazaki K and Hirth G (2016) Dehydration of lawsonite could directly trigger earthquakes in subducting oceanic crust. *Nature* **530**, 81–4.
- Otsuki K, Monzawa N and Nagase T (2003) Fluidization and melting of fault gouge during seismic slip: identification in the Nojima fault zone and implications for local earthquake mechanisms. *Journal of Geophysical Research* **108**, B4, doi: [10.1029/2001JB1711](https://doi.org/10.1029/2001JB1711).
- Ozawa K and Takizawa S (2007) Amorphous material formed by the mechanochemical effect in natural pseudotachylyte of crush origin: a case study of the Iida-Matsuwaka Fault, Nagano Prefecture, Central Japan. *Journal of Structural Geology* **29**, 1855–69.
- Passchier CW and Trouw RAJ (1996) *Microtectonics*. Berlin: Springer-Verlag.
- Pec M, Stünitz H, Heilbronner R, Dury M and DE Capitani, C (2012) Origin of pseudotachylytes in slow creep experiments. *Earth and Planetary Science Letters* **355**, 299–310.
- Pelletier L and Müntener O (2006) High pressure metamorphism of the Lanzo peridotite and its oceanic cover, and some consequences for the Sesia-Lanzo zone (northwestern Italian Alps). *Lithos* **90**, 111–30.
- Philpotts AR (1964) Origin of pseudotachylytes. *American Journal of Science* **262**, 1008–35.
- Price NA, Johnson SE, Gerbi CC and West DP Jr (2012) Identifying deformed pseudotachylyte and its influence on the strength and evolution of a crustal shear zone at the base of the seismogenic zone. *Tectonophysics* **518–521**, 63–83.
- Prieto GA, Florez M, Barrett SA, Beroza GC, Pedraza P, Blanco JF and Poveda E (2013) Seismic evidence for thermal runaway during intermediate-depth earthquake rupture: seismic evidence for thermal runaway. *Geophysical Research Letters* **40**, 6064–8.
- Ravna EJK, Andersen TB, Jolivet L and De Capitani C (2010) Cold subduction and the formation of lawsonite eclogite-constraints from prograde evolution of eclogitized pillow lava from Corsica. *Journal of Metamorphic Geology* **28**, 381–95.
- Ray SK (2004) Melt-clast interaction and power-law size distribution of clasts in pseudotachylytes. *Journal of Structural Geology* **26**, 1831–43.
- Rowe CD, Kirkpatrick JD and Brodsky EE (2012) Fault rock injections record paleo-earthquakes. *Earth and Planetary Science Letters* **335–336**, 154–66.
- Rowe CD, Moore JC and McKeiman AW (2005) Large-scale pseudotachylytes and fluidized cataclases from an ancient subduction thrust fault. *Geology* **33**, 937–40.
- Scambelluri M, Pennacchioni G, Gilio M, Bestmann M, Plümper O and Nestola F (2017) Fossil intermediate-depth earthquakes in subducting slabs linked to differential stress release. *Nature Geosciences* **10**, 960–6, doi: [10.1038/s41561-017-0010-7](https://doi.org/10.1038/s41561-017-0010-7).
- Schenk V (1980) U-Pb and Rb-Sr radiometric dates and their correlation with metamorphic events in the granulite-facies basement of the Serre, southern Calabria (Italy). *Contributions to Mineralogy and Petrology* **73**, 23–38.
- Shimabukuro DH, Wakabayashi J, Alvarez W and Chang SC (2012) Cold and old: the rock record of a subduction initiation beneath a continental margin, Calabria, southern Italy. *Lithosphere* **4**, 524–32.
- Sibson RH (1975) Generation of pseudotachylyte by ancient seismic faulting. *The Geophysical Journal of the Royal Astronomical Society* **43**, 775–94.
- Sibson RH and Toy VG (2006) The habitat of fault-generated pseudotachylyte: presence vs. absence of friction-melt. In *Earthquakes: Radiated Energy and the Physics of Faulting* (eds R Abercrombie, A McGarr, H Kanamori and G Di Toro), pp. 153–66. Washington, DC: American Geophysical Union, Geophysical Monograph no. 170.
- Spray JG (2010) Frictional melting processes in planetary materials: from hyper-velocity impacts to earthquakes. *Annual Review of Earth and Planetary Sciences* **38**, 221–54.
- Stewart CA and Miranda EA (2017) The rheological evolution of brittle-ductile transition rocks during the earthquake cycle: evidence for a ductile precursor to pseudotachylyte in an extensional fault system, South Mountains, Arizona. *Journal of Geophysical Research Solid Earth* **122**, 10643–65.

- Takagi H, Goto K and Shigematsu N** (2000) Ultramylonite bands derived from cataclasite and pseudotachylite in granites, northeast Japan. *Journal of Structural Geology* **22**, 1325–39.
- Theunissen K, Smirnova L and Dehandschutter B** (2002) Pseudotachylites in the southern border fault of the Cenozoic intracontinental Teletsk basin (Altai, Russia). *Tectonophysics* **351**, 169–80.
- Toyoshima T** (1990) Pseudotachylite from the main zone of the Hidaka metamorphic belt, Hokkaido, northern Japan. *Journal of Metamorphic Geology* **8**, 507–23
- Ujiie K, Yamaguchi A, Kimura G and Toh S** (2007) Fluidization of granular material in a subduction thrust at seismogenic depths. *Earth and Planetary Science Letters* **259**, 307–18.
- Vitale S and Ciarcia S** (2013) Tectono-stratigraphic and kinematic evolution of the southern Apennines/Calabria-Peloritani Terrane system (Italy). *Tectonophysics* **583**, 164–82.
- Vitale S, Ciarcia S, Fedele L and Tramparulo FDA** (2019) The Ligurian oceanic successions in southern Italy: the key to decrypting the first orogenic stages of the southern Apennines-Calabria chain system. *Tectonophysics* **750**, 243–61, doi: [10.1016/j.tecto.2018.11.010](https://doi.org/10.1016/j.tecto.2018.11.010).
- Vitale Brovarone A, Beyssac O, Malavieille J, Molli G, Beltrando M and Compagnoni R** (2013) Stacking and metamorphism of continuous segments of subducted lithosphere in a high-pressure wedge: the example of Alpine Corsica (France). *Earth-Science Reviews* **116**, 35–6.
- Wang H, Li H, Janssen C, Sun Z and Si J** (2015) Multiple generations of pseudotachylite in the Wenchuan fault zone and their implications for coseismic weakening. *Journal of Structural Geology* **74**, 159–71.
- Wang H, Li H, Si J, Sun Z & Huang Y** (2014) Internal structure of the Wenchuan earthquake fault zone, revealed by surface outcrop and WFSD-1 drilling core investigation. *Tectonophysics* **619–620**, 101–14.
- Wenk HR, Johnson LR and Ratschbacher L** (2000) Pseudotachylites in the Eastern Peninsular Ranges of California. *Tectonophysics* **321**, 253–77.
- Wex S, Mancktelow NS, Hawemann F, Camacho A and Pennacchioni G** (2017) Geometry of a large-scale, low-angle, midcrustal thrust (Woodroffe Thrust, central Australia). *Tectonics* **36**, 2447–76.
- Zheng Y, Li H, Sun Z, Wang H, Zhang J, Li C and Cao Y** (2016) New geochronology constraints on timing and depth of the ancient earthquakes along the Longmen Shan fault belt, eastern Tibet. *Tectonics* **35**, 2781–806.